# A Broadband Patch Antenna With Tripolarization Using Quasi-Cross-Slot and Capacitive Coupling Feed

Yi Zhang, *Student Member, IEEE*, Kunpeng Wei, *Student Member, IEEE*, Zhijun Zhang, *Senior Member, IEEE*, and Zhenghe Feng, *Fellow, IEEE*

***Abstract*—This letter presents a novel design of patch antenna with quasi-cross-slot and capacitive coupling feeding to achieve tripolarization with high isolation over a wide bandwidth. Two degenerate $\mathrm{TM}_{11}$ modes and one $\mathrm{TM}_{01}$ mode of the circular patch antenna are generated to realize three orthogonal polarizations. By using the proposed quasi-cross-slots, good measured isolations (better than 20 dB) were obtained. The measured impedance bandwidths of the proposed antenna ports are 2.13–2.58, 2.13–2.43, and 2.13–2.58 GHz, respectively. Details of the proposed design and measured results are presented and discussed.**

***Index Terms*—Cross slot, patch antenna, polarization diversity, tripolarization.**

## I. Introduction

During the last several years, wireless communication systems have been increasing rapidly. Multiple-input–multiple-output (MIMO) technology has been used to improve wireless system performance. Polarization diversity plays an important role in the MIMO system for combating the multipath propagation effects or enhancing the capacity of the system performance [1], [2]. In the urban or the indoor wireless environment, after complicated multiple reflections or scatterings, the polarization of the propagating radio wave may become diversified. To enhance system performance, an antenna with polarization diversity is an excellent choice.

Many efforts have been made to achieve the dual-polarized patch antennas [3]–[7]. In general, two orthogonal modes are excited to achieve dual polarizations, and the design structure includes two orthogonal offset slots [3], cross-shaped slots [4], [5], or H-shaped slots [6]. Moreover, hybrid feeding technique was used to achieve dual polarizations [7], [8]. For example, in [8], the designers used the H-shaped slot to excite the broadside mode and the capacitive coupling feeding to excite the monopole mode, and dual polarizations were obtained.

To make full use of the polarization diversity, the antennas with the tripolarization characteristic were studied in [9]–[12]. There were several methods to achieve tripolarization. In [9], the two orthogonal slots and a monopole are adopted. The dielectric resonator antenna (DRA) for two orthogonal polarizations and a monopole for the third polarization are proposed in [10]. To reduce the profile of the tripolarization antenna, a disk-loaded monopole was used in the design of [11] and [12] instead of a single monopole. Two degenerate $\mathrm{TM}_{11}$ modes were fed by the two orthogonal H-shaped slots. They used the disk-loaded monopole for the third polarization to reduce the profile. In their designs, two orthogonal patch modes were employed to realize the broadside pattern, and the monopole mode was used to radiate conical pattern. Although these designs effectively reduce the profile of the antennas, the operating bandwidths are not sufficient. The measured $-6$-dB impedance bandwidths are only 2.35–2.52, 2.34–2.54, and 2.38–2.49 GHz for the three ports [12].

This letter proposes a broadband conformal patch antenna with tripolarization for MIMO application. To achieve a broad impedance bandwidth while maintaining good isolations among the patch antenna ports, a quasi-cross-slot and capacitive coupling feed is used in the proposed design. The prototype antenna was fabricated and measured. The antenna has a simple structure and a compact size, and the measured results can validate the theoretical simulation.

## II. Antenna Design

The geometry with detailed dimensions of the proposed antenna is illustrated in Fig. 1. The upper and the bottom layers are fabricated on a Teflon ($\varepsilon_{\mathrm{r}} = 2.65$, $\tan\delta = 0.002$) substrate with a thickness of 0.5 mm. The driven rod in the middle of the antenna, which connects the two layers, is a circular tube with an outer radius of $r1$. The dimensions of the ground plane on the bottom layer are $l_{\mathrm{g}} \times l_{\mathrm{g}}$. The annular radiating patch on the upper layer has an outer radius of $r3$ and an inner radius of $r1$, which is supported by the driven rod with a height of $h$.

Ports 1 and 3 are fed by the quasi-cross-shaped slot etched on the ground and symmetrically centered below the radiating patch. Two orthogonal $\mathrm{TM}_{11}$ modes with broadside radiation patterns are excited. The current distributions are shown in

Manuscript received June 14, 2013; accepted June 21, 2013. Date of publication July 04, 2013; date of current version July 25, 2013. This work was supported by the National Basic Research Program of China under Contract 2010CB327400, in part by the Qualcomm, Inc. under Contract 2009AA011503, the Qualcomm, Inc. under Contract 61271135, the National Science and Technology Major Project of the Ministry of Science and Technology of China 2010ZX03007-001-01, and Qualcomm, Inc.

Y. Zhang is with State Key Laboratory on Microwave and Digital Communications, Tsinghua National Laboratory for Information Science and Technology, Department of Electronic Engineering, Tsinghua University, Beijing 100084, China, and also with Zhengzhou Information Science and Technology Institute, Zhengzhou 450002, China.

K. Wei, Z. Zhang, and Z. Feng are with the State Key Laboratory on Microwave and Digital Communications, Tsinghua National Laboratory for Information Science and Technology, Department of Electronic Engineering, Tsinghua University, Beijing 100084, China (e-mail: zjzh@tsinghua.edu.cn).

Color versions of one or more of the figures in this letter are available online at http://ieeexplore.ieee.org.

Digital Object Identifier 10.1109/LAWP.2013.2271782

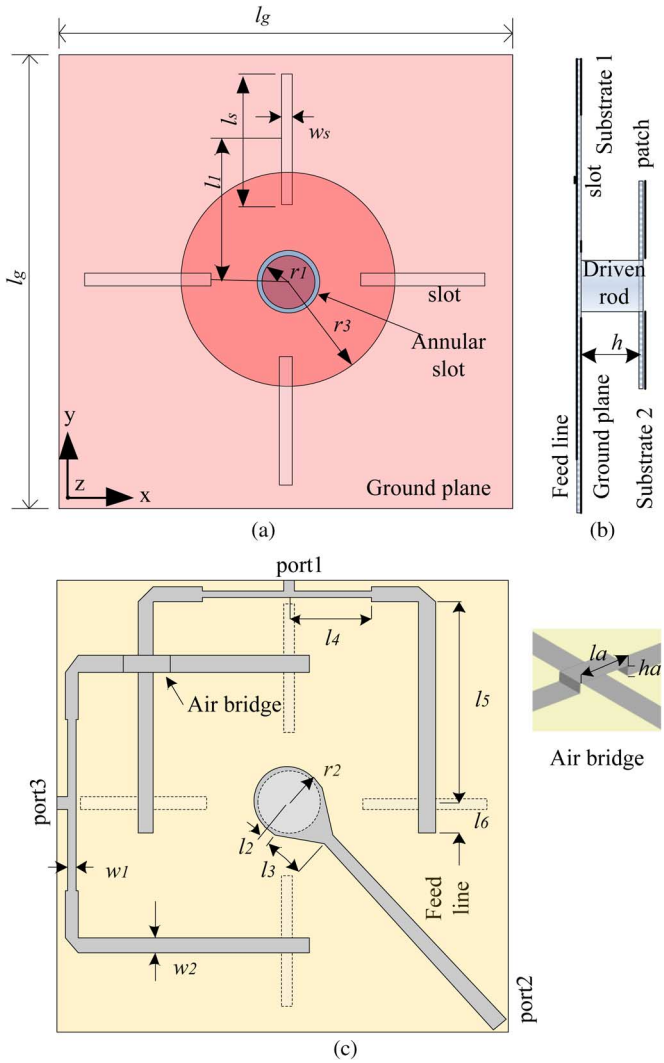


Fig. 1. Geometry of the proposed antenna. (a) Top view. (b) Side view. (c) Bottom view.

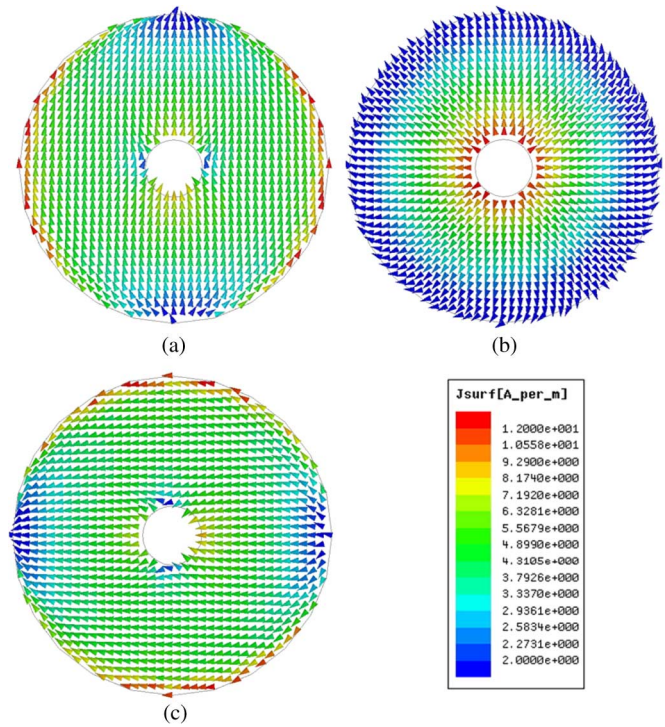


Fig. 2. Currents distribution with different ports being excited: (a) port 1, (b) port 2, and (c) port 3.

TABLE I
DIMENSIONS OF THE PROPOSED ANTENNA (UNIT: MILLIMETER)

| *lg* | *h* | *ls* | *ws* | *r1* | *r2* | *r3* | *w1* | *w2* |
|---|---|---|---|---|---|---|---|---|
| 120 | 9.5 | 33 | 2 | 5 | 6 | 6.4 | 0.8 | 1.4 |
| *l1* | *l2* | *l3* | *l4* | *l5* | *l6* | *la* | *ha* | |
| 28.5 | 2.4 | 6 | 20 | 56.6 | 5 | 4 | 0.5 | |

Fig. 2(a) and (c) when ports 1 and 3 are excited, respectively. The direction of the currents with port 1 that has been excited is along the $y$-axis, while it is along $x$-axis when port 3 is excited. Hence, two orthogonal polarizations are obtained, and the broadside radiation patterns are observed for the same direction at the edges of the radiating patch.

The impurity of two linear polarizations and coupling between two orthogonal polarizations can be overcome by using a quasi-cross-shaped slot. The coupling slots are of dimensions $l_s \times w_s$, with a distance of $l1$ to the center of the patch. The two ports are connected through a transmission line, which have two transmission arms to excite the slots, respectively. In the end of the transmission line, a tuning stub with a length of $l6$ is used to tune resonance frequency. A section of the transmission line with dimensions of $l4 \times w1$ is used to make the impedance match with the port. An air bridge is used in the cross section of the two transmission arms.

A $\mathrm{TM}_{01}$ mode with monopole radiation pattern is observed when port 2 is excited. The current distribution is shown in Fig. 2(c). It is clearly seen that the direction of the current on the radiating patch is radial in the $\mathrm{TM}_{01}$ mode. The conical radiation pattern is obtained for the $\mathrm{TM}_{01}$ mode with the polarization along $z$-axis. From the circular cavity model, the resonant frequency of the $\mathrm{TM}_{01}$ is about twice that of the $\mathrm{TM}_{11}$. To overlap the operating bandwidth of the three ports, a capacitive coupled feed with a driven rod and an annual gap is applied to shift down the resonant frequency of the $\mathrm{TM}_{01}$ mode. This port is excited through a quasi-circular open stub, which has a gradual broadband impedance transformation and a transmission line with an impedance of 50 Ω. The driven rod couples the electromagnetic energy to the radiating patch through an annular gap on the ground. The impedance bandwidth can be improved by enlarging the radius of the driven rod. The annual gap between the driven rod and the ground is capacitive, which can compensate the inductive effect by the driven rod [8]. All configuration parameters for the proposed antenna are shown in Table I.

## III. Simulation and Measurement Results

The proposed antenna structure is designed and analyzed by using the Ansoft High Frequency Structure Simulator (HFSS).

### *A. Parametric Study of the Proposed Antenna*

Fig. 3 shows the simulated results of return loss of the ports with different heights $h$ of the driven rod, which shows a strong

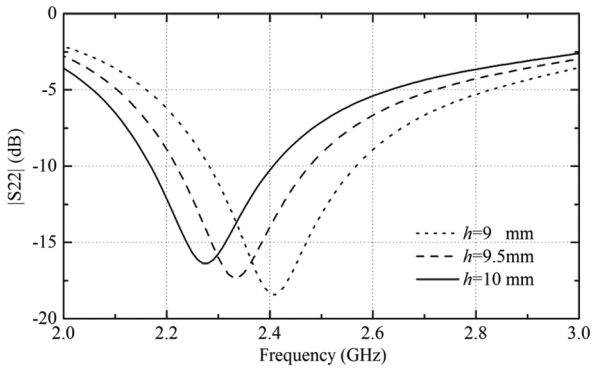


Fig. 3. Simulated reflection coefficients of the port 2 for $h = 9, 9.5$, and 10 mm.

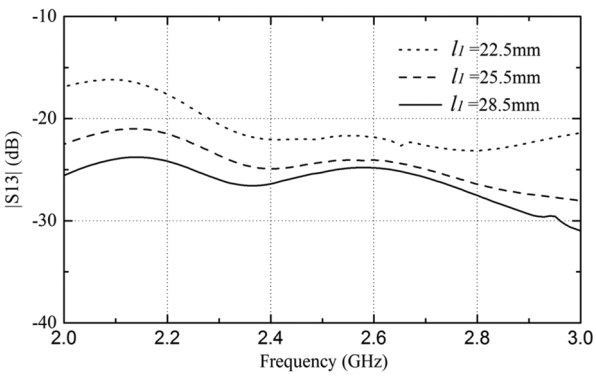


Fig. 4. Simulated isolation between ports 1 and 3 for $S_1 = 22.5, 25.5$, and 28.5 mm.

relationship with resonant frequency. As $h$ increases, the resonant frequency of the port 2 is shifted down, while the resonant frequency of port 1 or 3 is stable, which is not shown for brevity. This is because that the resonant point of the excited conical mode with port 2 is decided by the length of $(h + r_3)$. However, the resonant frequencies of the $\mathrm{TM}_{11}$ modes depend on the $r_3$.

Fig. 4 shows the simulated results of the isolation between ports 1 and 3 with variations of $l_1$. In general, better isolation results are available when the excited field is more symmetrical. When $l_1$ is small, strong coupling will occur between the ports. The space between two slots, which are adjacent and orthogonal, should be as big as possible to obtain high isolation. However, if $l_1$ is large, the coupling of the upper patch and the feeding slots is too weak, which would decrease the impedance bandwidth. For compromise, we chose the value of $l_1$ as 28.5 mm in our design. Furthermore, the isolations between ports 2 and 1 or 3 are almost not varied, while $l_1$ has been changed.

### B. Measurement Results

To verify the simulated design, an antenna prototype was fabricated and tested. The photographs of the prototype are shown in Fig. 5.

The measured and the simulated return losses are shown in Fig. 6. It is clearly seen that the measured data of return losses of the three ports are in good agreement with the simulated results.

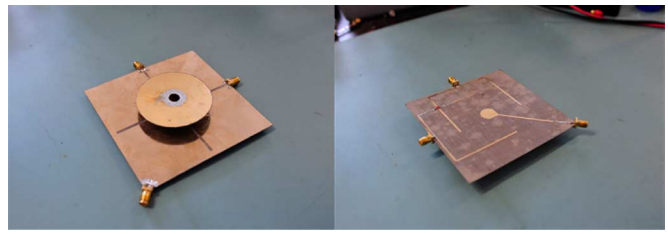


Fig. 5. Prototype of the proposed antenna: (a) top view and (b) back view.

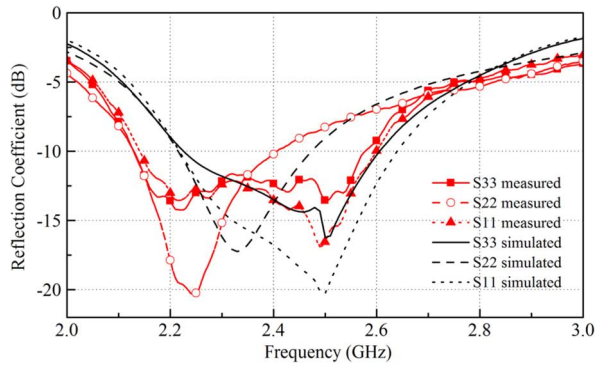


Fig. 6. Measured and simulated return loss of each port.

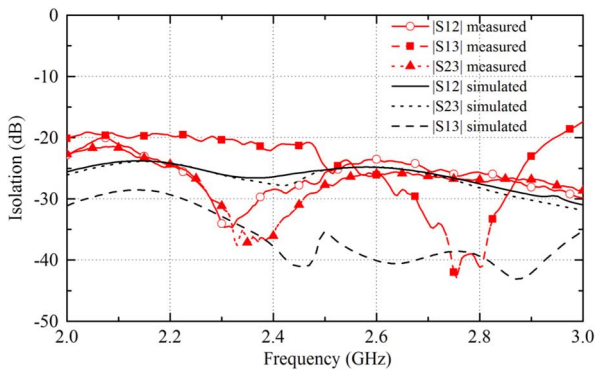


Fig. 7. Measured and simulated isolation between each two ports.

The small discrepancy might be caused by the manufacturing tolerance. For example, the $-10$-dB measured impedance bandwidth of port 2 is from 2.13 to 2.43 GHz, while the simulated impedance bandwidth is from 2.22 to 2.5 GHz. This is because the height of $h$ in the manufacturing process is higher than the simulation parameter. The $-10$-dB measured impedance bandwidth of the other ports is from 2.13 to 2.58 GHz.

The measured and the simulated isolations between each of the two ports are shown in Fig. 7. The measured results are in accordance with the simulated results. The simulated isolations are better than $-25$ dB in the impedance bandwidth. The isolation between ports 1 and 3 in the measured results has deteriorated compared to the simulation. However, the result is better than $-20$ dB in the impedance bandwidth.

The measured and the simulated radiation patterns at 2.34 GHz are shown in Fig. 8. It is worth mentioning here that when the radiation pattern is measured for exciting each port, we must ensure the other ports are matched with 50-$\Omega$ loads. Good agreement between the simulated and the measured

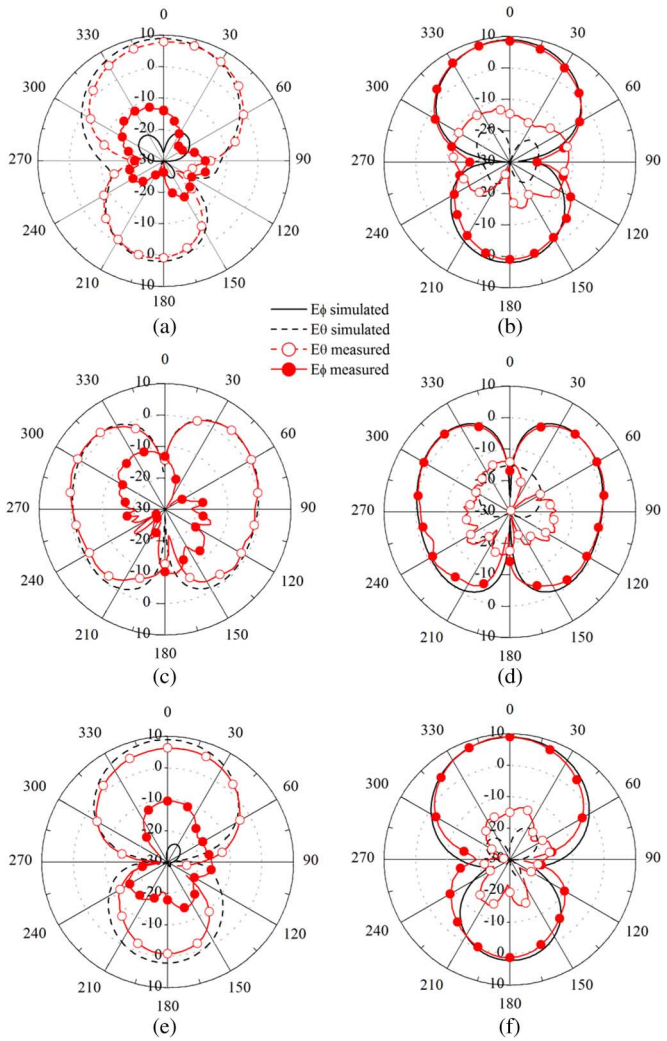


Fig. 8. Measured and simulated gain patterns of the proposed antenna. (a) Port 1, $xz$-plane. (b) Port 1, $yz$-plane. (c) Port 2, $xz$-plane. (d) Port 2, $yz$-plane. (e) Port 3, $xz$-plane. (f) Port 3, $yz$-plane.

results is obtained. For ports 1 and 3, the good broadside patterns are obtained for microstrip antenna radiation. The cross polarizations are better than −20 dB. The monopole-like radiation pattern is obtained for port 2. There is some discrepancy between the radiation patterns of the cross polarization, which should be the causes of the test cable and the driven rod being unparallel to the test polarization.

Fig. 8 also shows the gains of measured and simulated at 2.34 GHz. Measured gains of ports 1 and 3 are about 8.6 dBi for broadside radiation with quasi-cross-shaped slot feeding. The measured gain of the port 2 is about 3.2 dBi for monopole-like radiation. The slight decrease in measured gains, compared to the simulated results, might be the cause of the conducting loss and the loss of the SMA connectors.

## IV. Conclusion

A broadband patch antenna with tripolarization by using a quasi-cross-slot and capacitive coupling feed has been demonstrated. By using the quasi-cross-slot, good isolation performances (better than −20 dB) have been obtained. Parameters in the design have been studied. The measured −10-dB impedance bandwidths for three ports are 2.13–2.58, 2.13–2.43, and 2.13–2.58 GHz, respectively. The measured gains of the two ports for broadside radiation are 8.6 dBi. The gain of port 2 for monopole-like radiation can reach about 3.2 dBi.

## References

[1] N. K. Das, T. Inoue, T. Taniguchi, and Y. Karasawa, "An experiment on MIMO system having three orthogonal polarization diversity branches in multipath-rich environment," in *Proc. 60th IEEE Veh. Technol Conf.*, Sep. 2004, vol. 2, pp. 1528–1532.

[2] E. R. Iglesias, O. Q. Teruel, and M. S. Ferflifldez, "Compact multimode patch antennas for MIMO applications," *IEEE Antennas Propag. Mag.*, vol. 50, no. 2, pp. 197–205, Apr. 2008.

[3] A. Adrian and D. H. Schaubert, "Dual aperture-coupled microstrip antenna for dual or circular polarization," *Electron. Lett.*, vol. 23, no. 23, pp. 1226–1228, Nov. 1987.

[4] M. Barba, "A high-isolation, wideband and dual-liear polarization patch antenna," *IEEE Trans. Antennas Propag.*, vol. 56, no. 5, pp. 1472–1476, May 2008.

[5] J. Lu, Z. Kuai, X. Zhu, and N. Zhang, "A high-isolation microstrip patch antenna with quasi-cross-shaped coupling slot," *IEEE Trans. Antennas Propag.*, vol. 59, no. 7, pp. 2713–2717, Jul. 2011.

[6] K. L. Wong, H. C. Tung, and T. W. Chiou, "Broadband dual-polarized aperture-coupled patch antenna with modified H-shaped coupling slots," *IEEE Trans. Antennas Propag.*, vol. 50, no. 2, pp. 188–191, Feb. 2002.

[7] I. Acimovic, D. A. McNamara, and A. Petosa, "Dual-polarized microstrip patch planar array antennas with improved port-to-port isolation," *IEEE Trans. Antennas Propag.*, vol. 56, no. 11, pp. 3433–3439, Nov. 2008.

[8] K. Wei, Z. Zhang, W. Chen, and Z. Feng, "A novel hybrid-fed patch antenna with pattern diversity," *IEEE Antennas Wireless Propag. Lett.*, vol. 9, pp. 562–565, 2010.

[9] K. Itoh, R. Watanabe, and T. Matsumoto, "Slot-monopole antenna system for energy-density reception at UHF," *IEEE Trans. Antennas Propag.*, vol. AP-27, no. 4, pp. 485–489, Jul. 1979.

[10] D. Gray and T. Watanabe, "Three orthogonal polarization DRA-monopole ensemble," *Electron. Lett.*, vol. 39, no. 10, pp. 766–767, May 2003.

[11] H. Zhong, Z. Zhang, W. Chen, Z. Feng, and M. F. Iskander, "A tripolarization antenna fed by proximity coupling and probe," *IEEE Antennas Wireless Propag. Lett.*, vol. 8, pp. 465–467, 2009.

[12] X. Gao, H. Zhong, Z. Zhang, Z. Feng, and M. F. Iskander, "Low-profile planar tripolarization antenna for WLAN communications," *IEEE Antennas Wireless Propag. Lett.*, vol. 9, pp. 83–86, 2010.